Vacuum beat wave acceleration

B. Hafizi
Icarus Research, Inc., P.O. Box 30780, Bethesda, Maryland 20824-0780
and Omega-P, Inc., P.O. Box 2008, New Haven, Connecticut 06520-2008

A. Ting, E. Esarey, P. Sprangle, and J. Krall
Plasma Physics Division, Naval Research Laboratory, Washington, D.C. 20375
(Received 31 July 1996)

A vacuum beat wave accelerator (VBWA), in which two focused laser beams of differing wavelengths generate a beat wave that can impart a net acceleration to particles, is analyzed and simulated. The mechanism relies on the ponderomotive ($\mathbf{v}\times\mathbf{B}$) force, thus circumventing the so-called Lawson-Woodward theorem. No gas, plasma, or other proximate material medium is required to achieve a net energy gain. The single-stage energy gain of the VBWA is limited by diffraction of the laser beams, particle slippage, and radial walkoff. In the simulations the particles are synchronous with the beat wave for a short interval of time and the energy gain has the nature of an impulse delivered near the focal region. Simulations show that the problem of radial walkoff may be ameliorated by using a converging beam of particles, as naturally occurs for injection of a finite-emittance beam. For terawatt-level laser beams, with wavelengths 1 μm and 0.5 μm, and a 4.5 MeV finite-emittance electron beam, the energy can be increased to $\sim$12.5 MeV in a nonsynchronous interaction over a distance of under 4 mm, with a peak acceleration gradient $\sim$15 GeV/m and an estimated trapping fraction of $\sim$1%. The simulated energy gain is compared with analytical predictions. Scaling is illustrated by increasing the injection energy to 50 MeV. [S1063-651X(97)03704-5]

PACS number(s): 29.27.−a

I. INTRODUCTION

Advances in the development of high power lasers continue to spur new concepts for accelerators [1]. There is a need for radically new approaches with the potential for acceleration gradients considerably larger than the $\sim$100 MeV/m typical of proposed next-generation X-band linacs. Energetic electrons have been observed in a number of laser-driven plasma beat wave and wakefield experiments [2–9] and peak gradients of $\sim$100 GV/m have been inferred [7]. If such an acceleration gradient could be sustained for $\sim$10 m, a TeV electron beam would be produced. This would essentially remove site development problems associated with conventional acceleration schemes. However, laser-based plasma acceleration schemes face a myriad of challenges that must be overcome before any of these schemes can be considered practical. Some of the difficulties lie in the fact that the plasma (or gas) medium, needed to support the accelerating slow waves, may be susceptible to instability or induce scattering. Additionally, since acceleration of positrons is a *sine qua non* in lepton colliders, their rapid annihilation in a plasma or gas could be problematic.

An alternative approach to particle acceleration is to make use of laser beams *in vacuo* in the far-field limit, i.e., in regions that are far (compared to the vacuum wavelength) from boundaries [10–18], thus mitigating material breakdown, plasma formation, and instability. Particle acceleration *in vacuo* by laser fields can be divided into two main categories: (i) direct acceleration, in which the accelerating force is linearly proportional to the field, and (ii) ponderomotive acceleration, in which the accelerating force is proportional to the square of the field.

The simplest method for direct acceleration utilizes a single laser beam. Plane electromagnetic waves are not suitable for direct acceleration since the longitudinal electric field component (along the direction of propagation, taken to be the z axis) is zero. In three dimensions, however, a focused laser beam will have a finite longitudinal component. It follows from Gauss's theorem that, in general, the longitudinal field E_z is related to the (dominant) transverse electric field $\mathbf{E}_\perp$ through $\partial E_z/\partial z=-\boldsymbol{\nabla}_\perp\cdot\mathbf{E}_\perp$, where the suffix $\perp$ denotes the transverse component. Higher order Gaussian beams, in which $\mathbf{E}_\perp$ is zero along the z axis and E_z is nonzero, have been analyzed as possible candidates for vacuum laser acceleration [10–16]. Alternatively, a similar electric field configuration near the z axis can be produced by intersecting two laser beams at finite angle [13–15].

The existence of a longitudinal electric field is not sufficient for a viable acceleration scheme. It is also necessary to ensure that the accelerating field can interact with the particles synchronously over an extended distance. In particular, the phase velocity β_{ph} of the accelerating field must be close to the longitudinal particle velocity β_z over a sufficiently long interaction distance, where $\boldsymbol{\beta}=\mathbf{v}/c$ denotes a velocity $\mathbf{v}$ normalized to the speed of light *in vacuo*. In the absence of phase matching, particles slip relative to the laser field, limiting the distance over which acceleration takes place. In far-field accelerators phase slippage occurs because the longitudinal phase velocity of the laser beam *in vacuo* exceeds c. In addition, β_{ph} and β_z vary along the particle trajectory and, hence, the phase relationship between the particle and the wave evolves continuously. In fact, it is possible to show that if a highly relativistic particle ($v_z=c$) interacts with the longitudinal laser field from $z=-\infty$ to $z=\infty$ *in vacuo* the net

energy gain is zero. This is the essence of the Lawson-Woodward theorem [12–14,19,20].

In ponderomotive laser acceleration configurations, on the other hand, the phase velocity can be subluminous and particle acceleration over an extended range is, in principle, possible. This is the case in the vacuum beat wave accelerator (VBWA) [13,14], which utilizes a pair of laser beams to accelerate particles. The VBWA is similar to the inverse free-electron laser (IFEL), wherein a propagating electromagnetic wave interacts with an electron beam in the presence of a periodic magnetostatic field, and the resulting beat wave produces acceleration. The VBWA is a novel variant of this concept, utilizing instead two laser beams to form a beat wave to accomplish the same task. With the use of powerful lasers, such as table-top terawatt (T^3) lasers [21], the VBWA promises to be a more compact, or higher-gradient, accelerator than the IFEL. Since the VBWA does not require the proximity of a material medium, nor does it take place in a plasma, it is limited neither by material breakdown (as in an inverse Cerenkov accelerator) nor by pair annihilation of positrons (as in plasma beat wave or plasma wakefield accelerators).

The ponderomotive force of a single, linearly polarized laser pulse can lead to scattering of particles, as demonstrated in Ref. [17]. The phase velocity of this ponderomotive force exceeds c since the phase velocity of a single laser pulse is greater than c. Thus the phase synchronism necessary for high energy acceleration is not obtained. For ultrashort laser pulses there is an additional longitudinal ponderomotive force that arises from gradients in the laser pulse envelope. The phase velocity of the ponderomotive force associated with the envelope is approximately equal to the group velocity v_g of the pulse, which can be less than c [18]. The ponderomotive force associated with variations in the envelope is less than that associated with variations in the *phase* by λ/L, where λ is the wavelength and L is the pulse length. Consequently, the energy gain resulting from the envelope variation is relatively small. In the following it is assumed that $L\rightarrow\infty$. As further justification, we note that the distance over which a relativistic particle slips with respect to the laser pulse—which travels at v_g—is much less than the laser pulse length L.

In this paper earlier models [13,14] of the VBWA are extended in order to better represent the detailed motion of the particles, as observed in simulations. The parameters of the simulations are chosen to correspond to those of an experiment to be performed at the Naval Research Laboratory. Simulations demonstrate that, for low energies and on-axis injection of particles, the VBWA is limited by slippage. Additionally, they reveal that the VBWA interaction has the characteristics of an impulse, delivered to the particles in the vicinity of the focal point. New analytical estimates for the energy gain, appropriate to an impulsive interaction, are obtained. Concomitant with acceleration, the impulse scatters particles in the transverse plane. It is demonstrated that by employing converging particle beams—that come to a focus at the same location as the laser beams—radial walkoff is mitigated and a several fold increase in energy is possible with TW-level laser beams. Simulation results are also presented to show the scaling of the VBWA to higher injection energies.

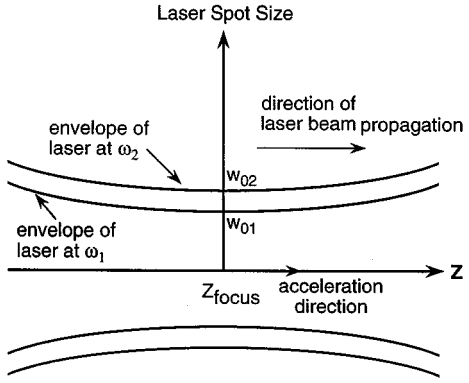

FIG. 1. Vacuum beat wave accelerator configuration. Two collinear and copropagating laser beams come to a common focus at $Z_{\rm focus}$. The waist of the laser beam of frequency ω_1 (ω_2) is $w_{0,1}$ ($w_{0,2}$).

II. PONDEROMOTIVE BEAT WAVE

In the presence of an electromagnetic field *in vacuo* the change in the relativistic factor γ of an electron of mass m and charge e, moving along the z axis, due to the longitudinal component of the laser field E_z, is given by

$$\Delta\gamma=-\frac{|e|}{mc^2}\int_{-l}^{l}dt\ v_zE_z.$$

The usual expression of the Lawson-Woodward theorem states that $\Delta\gamma=0$ in the ultrarelativistic limit ($v_z=c$) provided $l\rightarrow\infty$ [12–14,19,20]. Since the theorem specifically neglects the Lorentz force due to the magnetic field **B**, i.e., $-|e|\mathbf{v}\times\mathbf{B}$, it is natural to consider a configuration wherein this force is significant with a view to escaping the theorem's conclusion. The $\mathbf{v}\times\mathbf{B}$ force is also referred to as the ponderomotive force.

Consider two laser beams, with frequencies ω_1 and ω_2, respectively, that propagate along a common axis and come to a common focus at $z=Z_{\rm focus}$, as shown in Fig. 1. For definiteness circularly polarized laser beams are considered throughout. The vector potential of such a beam is expressible as

$$\mathbf{A}_j=\frac{A_{0j}w_{0j}}{w_j}\exp(-r^2/w_j^2)(\hat{\mathbf{e}}_x\cos\psi_j+\hat{\mathbf{e}}_y\sin\psi_j)+A_{zj}\hat{\mathbf{e}}_z, \tag{1}$$

where the suffix $j=1,2$ identifies the laser beam, $\omega_j=ck_j=2\pi/\lambda_j$ defines the wave number k_j and wavelength λ_j,

$$w_j(z)=w_{0j}[1+(z-Z_{\rm ocus})^2/Z_{Rj}^2]^{1/2}$$

is the spot size at z, w_{0j} is the waist (radius), $Z_{Rj}=\pi w_{0j}^2/\lambda_j$ is the Rayleigh range (i.e., the diffraction scale length *in vacuo*), A_{0j} is a constant and $\hat{\mathbf{e}}_x$, $\hat{\mathbf{e}}_y$, and $\hat{\mathbf{e}}_z$ are unit vectors.

The expression for the vector potential, Eq. (1), is valid in the paraxial limit, where $w_{0j} \gg \lambda_j$. In Eq. (1), A_{zj} denotes the axial component of the vector potential. In the Coulomb gauge, div $\mathbf{A}_j=0$, whence $A_{zj}=O(A_{0j}/k_j w_j)$; i.e., A_{zj} is small compared to A_{0j} in the paraxial limit. The total vector potential is $\mathbf{A}=\mathbf{A}_1+\mathbf{A}_2$.

The vector potential for the lowest order Gaussian beam, Eq. (1), includes both a spot size variation and a phase variation. The phase ψ_j can be expressed as the sum of several physically distinct contributions

$$\psi_j=\psi_{pj}+\psi_{Gj}+\psi_{kj}+\psi_{0j}.$$

The first term, $\psi_{pj}=k_j z-\omega_j t$, is the usual plane wave phase. The second contribution, $\psi_{Gj}=-\tan^{-1}[(z-Z_{\rm focus})/Z_{Rj}]$, is due to the Guoy effect, which leads to an extra half-cycle of the phase shift upon passing through the focal region [22]. The third term, $\psi_{kj}=r^2(z-Z_{\rm focus})/(Z_{Rj}w_j^{\,2})$, is due to the curvature of the wave fronts and contributes for off-axis particles. The last term is an arbitrary constant.

As a first approximation, it is natural to assume that particles remain close to the axis, i.e., $r \ll w_{j0}$ through the interaction region. Therefore, disregarding the phase shift due to curvature, the Guoy effect causes the phase fronts of a Gaussian beam to shift forward by an extra π on passing through the waist and, hence, the phase velocity is slightly greater than c. The central idea in the VBWA is that the phase velocity of the beat wave of two laser beams may be controlled by appropriate choice of parameters, and, in fact, made sufficiently slow to trap particles.

Physically, beat wave acceleration may be important when the wiggle velocity of a particle in one of the laser beams, crossed into the magnetic field of the other beam, ''moves'' at a velocity that is close to that of the particle. We define auxiliary variables $\mathbf{u}=\mathbf{p}/(mc)$, where $\mathbf{p}=\gamma m\mathbf{v}$ is the momentum, and the normalized vector potential $\mathbf{a}=|e|\mathbf{A}/(mc^2)$. To lowest order in the fields and in the paraxial limit, $\mathbf{u}^{(0)}-\gamma^{(0)}\hat{\mathbf{e}}_z=\mathbf{a}+(u_0-\gamma_0)\hat{\mathbf{e}}_z$, where γ_0 and u_0 denote the initial values of the relativistic factor and of the axial component of $\mathbf{u}$, respectively, far upstream of the laser beams (where $\mathbf{a}\to\mathbf{0}$). Iterating, ponderomotive and diffractive effects enter the equations of motion at the next order,

$$\frac{d\gamma}{dz}=\frac{1}{2cu_z}\frac{\partial \mathbf{a}^2}{\partial t}+\frac{1}{c}\frac{\partial a_z}{\partial t}, \tag{2}$$

$$\frac{d\mathbf{u}_\perp}{dz}=\frac{d\mathbf{a}_\perp}{dz}-\frac{1}{2u_z}\boldsymbol{\nabla}_\perp \mathbf{a}^2-\boldsymbol{\nabla}_\perp \mathbf{a}_z, \tag{3}$$

where

$$\mathbf{a}^2=\hat{a}_1^2+\hat{a}_2^2+2\hat{a}_1\hat{a}_2\cos(\psi_2-\psi_1)+a_z^2, \tag{4}$$

$\hat{a}_j=(a_{0j}w_{0j}/w_j)\exp(-r^2/w_j^2)$ and $a_{0j}=|e|A_{0j}/(mc^2)$. Making use of Eq. (4) to evaluate the appropriate derivatives, Eqs. (2) and (3) become

$$\frac{d\gamma}{dz}=\frac{(k_2-k_1)\hat{a}_1\hat{a}_2}{u_z}\sin(\psi_2-\psi_1), \tag{5}$$

$$\begin{aligned}2u_z\frac{d(\mathbf{u}_\perp-\mathbf{a}_\perp)}{dz}\approx&-\boldsymbol{\nabla}_\perp[\hat{\mathbf{a}}_1^2+\hat{a}_2^2+(a_{z1}+a_{z2})^2]\\&-2\boldsymbol{\nabla}_\perp(\hat{a}_2\hat{a}_2)\cos(\psi_2-\psi_1)\\&+4\hat{a}_1\hat{a}_2\sin(\psi_2-\psi_1)\mathbf{r}(z-Z_{\rm focus})\\&\times\left(\frac{1}{Z_{R2}w_2^2}-\frac{1}{Z_{R1}w_1^2}\right),\end{aligned} \tag{6}$$

where $\mathbf{r}$ is the radius vector in cylindrical coordinates, and only the ponderomotive terms have been retained on the right hand sides of Eqs. (5) and (6). The normalized *beat wave* phase velocity is given by

$$\beta_{ph}^{-1}=1-\frac{1-(1-\hat{z}_2^2)r^2/w_2^2}{(k_2-k_1)Z_{R2}(1+\hat{z}_2^2)}+\frac{1-(1-\hat{z}_1^2)r^2/w_1^2}{(k_2-k_1)Z_{R1}(1+\hat{z}_1^2)}, \tag{7}$$

where $\hat{z}_j=(z-Z_{\rm focus})/Z_{\rm Rj}$ is the normalized axial coordinate relative to the focal point.

To complete the description of the slowly varying component of particle motion, Eqs. (5) and (6) must be supplemented by an equation for the variation of the beat wave phase

$$\begin{aligned}\frac{d(\psi_2-\psi_1)}{dz}=&(k_2-k_1)(\beta_{ph}^{-1}-\beta_z^{-1})+2\frac{\boldsymbol{\beta}_\perp\cdot\mathbf{r}}{\beta_z}(z-Z_{\rm focus})\\&\times\left(\frac{1}{Z_{R2}w_2^2}-\frac{1}{Z_{R1}w_1^2}\right),\end{aligned} \tag{8}$$

which follows from the definition of ψ_j.

III. ANALYTICAL ESTIMATES FOR ENERGY GAIN

To estimate the single stage energy gain in the VBWA the equations of motion are analyzed, extending previous models [13,14] of the interaction to account for the particle motion observed in the simulations. However, for these analytical studies the radial displacement of particles from the axis will be ignored for simplicity. It is further assumed that the motion is entirely determined by the beat wave, i.e., the individual laser fields are assumed to have no influence on the slow scale evolution of the particle energy. With these assumptions the motion is governed by the equation for the relativistic factor, Eq. (5), and that for the phase, Eq. (8).

Equation (8) permits one to identify a (local) slippage distance z_s, given by

$$z_s=\frac{\pi}{|(k_2-k_1)(\beta_{ph}^{-1}-\beta_z^{-1})|},$$

that is, a measure of the distance over which the phase of the particle in the beat wave slips by π. In terms of the slippage distance one is led to consider the following cases.

(a) *Synchronous acceleration*, $z_s/Z_{Rj} \gg 1$. Here the particle motion is such that it remains at a fixed phase with respect to the beat wave through the entire interaction region i.e., the relative phase $\psi_2-\psi_1=\psi_{\rm syn}=$const. This is referred to as the synchronous case, and the acceleration is simply limited by the axial falloff of the laser fields on either side of the focal region. This limit was examined in Refs. [13] and [14], taking $Z_{R1}=Z_{R2}$. This example is particularly interesting since the Guoy phase contributions of the two laser beams cancel out and, for an ultrarelativistic, *on-axis* particle, the relative phase $\psi_2-\psi_1=\psi_{0,2}-\psi_{0,1}$ is manifestly constant. Unfortunately, Eq. (7) shows that, when the Rayleigh ranges are set equal to one another, $\beta_{ph}=1$ and particles cannot maintain synchronism with the beat wave. This is also implied by Eq. (8). One way out of this dilemma is to assume that the Rayleigh ranges are unequal. If, without loss of generality, it is assumed that $Z_{R2}>Z_{R1}$, Eq. (5) may be integrated over the interval $(-\infty,\infty)$ to obtain the change in the relativistic factor

$$\Delta\gamma^2=4(k_2-k_1)Z_{R1}a_{0,1}a_{0,2}K(\sqrt{1-Z_{R1}^2/Z_{R2}^2})\sin\psi_{\rm syn}, \qquad (9)$$

where $K(x)$ is the complete elliptic integral of the first kind and $\beta_z\approx 1$ has been assumed. Maximum energy gain is obtained for $\psi_{\rm syn}=\pi/2$. When $Z_{R1}=Z_{R2}$ in Eq. (9), Eq. (48) of Ref. [14] is recovered.

The validity of synchronous acceleration may be checked by perturbing around the synchronous values of the relativistic factor, $\gamma_{\rm syn}(z)$ and the phase. Perturbing Eqs. (5) and (8), the equations of motion for the deviation $(\delta\gamma,\delta\psi)$ from the synchronous values are

$$\frac{d}{dz}\delta\gamma=-\frac{a_{0,2}a_{0,1}(k_2-k_1)}{\beta_{z,\rm syn}^3\gamma_{\rm syn}^2}\sin\psi_{\rm syn}\delta\gamma + \frac{a_{0,2}a_{0,1}(k_2-k_1)}{\beta_{z,\rm syn}\gamma_{\rm syn}}\cos\psi_{\rm syn}\delta\psi, \qquad (10)$$

$$\frac{d}{dz}\delta\psi=\frac{(k_2-k_1)\gamma_\perp^2}{(\beta_{z,\rm syn}\gamma_{\rm syn})^3}\delta\gamma. \qquad (11)$$

In writing Eqs. (10) and (11) use has been made of the definition $\gamma_\perp=(1+a^2)^{1/2}$ for the transverse relativistic factor [with $\gamma=\gamma_\perp\gamma_z\equiv\gamma_\perp(1-\beta_z^2)^{-1/2}$]. Additionally it has been assumed that the axial variation of the vector potential is sufficiently small, as quantified presently. It follows from Eqs. (10) and (11) that any deviation from the synchronous values evolves according to $\exp(\Gamma z)$, where

$$\Gamma\approx-\frac{a_{0,2}a_{0,1}(k_2-k_1)}{2\beta_{z,\rm syn}^3\gamma_{\rm syn}^2}\sin\psi_{\rm syn} \pm\left[\left(\frac{a_{0,2}a_{0,1}(k_2-k_1)}{2\beta_{z,\rm syn}^3\gamma_{\rm syn}^2}\sin\psi_{\rm syn}\right)^2 + \frac{(k_2-k_1)^2\gamma_\perp^2a_{0,2}a_{0,1}}{(\beta_{z,\rm syn}\gamma_{\rm syn})^4}\cos\psi_{\rm syn}\right]^{1/2}. \qquad (12)$$

Equation (12) indicates that acceleration is accompanied by phase bunching provided $\pi/2<\psi_{\rm syn}<\pi$. Equations (10)–(12) are valid provided the scale length for the variation of the vector potential (due to diffraction) is long compared with that for acceleration, which, in turn, is long compared with Γ^{-1}. That is, $\Gamma\gg|d\ln\gamma_{\rm syn}/dz|\gg|d\ln(a_j)/dz|$. Since $|d\ln(a_j)/dz|\sim|z-Z_{\rm focus}|/Z_{Rj}^2$, the second part of the inequality is valid in the focal region. However, examination of Eq. (12) reveals that $|\Gamma|$ is comparable to $|d\ln\gamma_{\rm syn}/dz|$ and, therefore, phase bunching is likely to be a slow process, taking place at the same rate as the acceleration. Thus synchronous acceleration is impractical because the beat wave phase velocity varies rapidly in the focal region.

(b) $\Delta\gamma/\gamma$ *small*, z_s/Z_{Rj} *arbitrary*. A different model of the interaction is obtained by assuming that the acceleration is weak; for example, a multistage system in which $\Delta\gamma/\gamma$ per stage is small. Analysis of this case proceeds by integrating Eq. (5)

$$\Delta\gamma^2=2(k_2-k_1)\,{\rm Im}\int_{-\infty}^{\infty}dz'\,\hat a_1(z')\hat a_2(z')\exp[i\Phi(z')], \qquad (13)$$

where

$$\Phi(z)=(k_2-k_1)\int^z dz'[\beta_{ph}^{-1}(z')-\beta_z^{-1}(z')] \qquad (14)$$

follows from Eq. (8) upon neglecting terms proportional to the transverse displacement. When the change in energy is small it is appropriate to make use of the Born approximation and take β_z to be a constant in Eq. (14). For equal Rayleigh ranges, $Z_{R1}=Z_{R2}=Z_R$, $\beta_{ph}=1$ and the evolution of the phase is readily determined from Eq. (14). Equation (13) then integrates to

$$\Delta\gamma^2=2\pi(k_2-k_1)Z_Ra_{0,1}a_{0,2}\exp(-\pi Z_R/z_s), \qquad (15)$$

where the constant of integration in Eq. (14) has been set equal to $\pi/2$. The interesting feature of Eq. (15) is the exponential factor. It reveals the manner in which slippage leads to phase mixing of the integral and reduces the acceleration gradient. The relevant dimensionless measure of slippage is clearly Z_R/z_s. Equation (15), however, underestimates the energy gain—at least in the numerical examples in Sec. IV—since it does not take into account the fact that in gaining energy the particles speed up and tend to catch up with the beat wave, effectively increasing z_s.

(c) *Impulse acceleration,* $z_s < Z_{Rj}$. The last model to be considered may be regarded to be the opposite extreme of case (a). Namely, one assumes that the phase variation is rapid compared to that of the amplitudes. In this case the acceleration is assumed to be significant in the immediate vicinity of the focal point. The rapid variation of the phase cuts off the integral in Eq. (13). The analysis, however, goes one step beyond case (b) by approximately correcting for the acceleration that takes place during the short interval around $Z_{\rm focus}$. Asymptotic evaluation of the integral in Eq. (13) proceeds by expanding the phase function in a Taylor series about $z = Z_{\rm focus}$

$$\Phi(z) = \Phi(Z_{\rm focus}) + (z - Z_{\rm focus})\Phi'(Z_{\rm focus}) + \tfrac{1}{2}(z - Z_{\rm focus})^2 \times \Phi''(Z_{\rm focus}) + \tfrac{1}{6}(z - Z_{\rm focus})^3 \Phi'''(Z_{\rm focus}) + \cdots .$$

In the highly relativistic limit and for equal Rayleigh ranges, $Z_{R1} = Z_{R2} = Z_R$, Eq. (13) reduces to

$$\Delta\gamma^2 \sim \frac{4\pi}{3}(k_2 - k_1) Z_R \frac{\gamma_\perp a_{0,1} a_{0,2}}{a} \times [J_{1/3}(b) + J_{-1/3}(b)] \sin\Phi(Z_{\rm focus}), \qquad (16)$$

where $b = (2\pi Z_R/3z_s)\gamma_\perp/a$, the amplitude a is given by Eq. (4) and $\gamma_\perp$ is defined following Eq. (11). The argument of the Bessel functions in Eq. (16) is also expressible as $b = (k_2 - k_1) Z_R \gamma_\perp^3/(3\gamma^2 a)$, and the Bessel function sum may alternatively be expressed in terms of the Airy function $\mathrm{Ai}(-(3b/2)^{2/3})$. Equation (16) may be useful in multistage systems, where $\Delta\gamma/\gamma$ per stage is relatively small.

Equations (9), (15), and (16) may be used to gain insight into the scaling properties of the VBWA [14]. The following observations may be made based on the form of these expressions. First, the energy gain is nearly proportional to the product of the amplitudes. As a result if either laser beam is weak (i.e., $a_{0,1} \ll 1$ or $a_{0,2} \ll 1$) the influence of the beat wave may be minor compared with that of the individual laser beams. Second, the scaling with the ratio of laser frequencies is more involved. At first sight the energy gain increases as $k_2 - k_1$ is increased. However, Eqs. (15) and (16) also depend on the slippage distance z_s, which decreases with increasing $k_2 - k_1$. As z_s decreases, the Bessel function sum in Eq. (16) decreases, reducing the energy gain. The optimal frequency ratio is therefore a function of several factors. Among these we should include the ease with which the two frequencies are generated in the laboratory; e.g., frequency doubling is typically straightforward. In any event, $\Delta\gamma \to 0$ as $k_2 - k_1 \to 0$. In this connection it should be noted that as b varies—due, for example, to an increase in the energy—the Bessel functions in Eq. (16) imply an oscillatory variation of $\Delta\gamma$. Accordingly, in a multistage system where the energy is to increase continuously, it may be necessary to gradually adjust the laser system parameters so as to avoid deceleration. Finally, to a first approximation, the energy gain is inversely proportional to the initial particle energy. That is, there is an energy beyond which the beat wave mechanism is not an effective method of acceleration since the laser power requirement becomes prohibitive. This property is shared by some other schemes, such as the inverse free-electron laser accelerator.

IV. NUMERICAL RESULTS

The expressions for the energy gain, Eqs. (9), (15), and (16), are approximate. They ignore the effects of the individual laser fields. Further, radial displacement of the particles is neglected and no information regarding beam emittance emerges. The latter is a serious shortcoming since the luminosity is directly related to beam emittance. There are three distinct transverse force terms in Eq. (6). The first arises from the ponderomotive effect of the two individual laser beams. These are always defocusing inasmuch as the laser intensity peaks on axis. The other two terms are due to the joint ponderomotive effect of the two beams. One would hope that there is a range of phase values such that $\sin(\psi_2 - \psi_1)$ positive, and therefore accelerating, while at the same time net focusing is obtained in the transverse direction.

For a comprehensive description one must seek a numerical solution where a finite-emittance beam of particles is injected along the z axis, copropagating with the laser beams towards the focus. The numerical method here employs a leapfrog integrator to push the particles in the prescribed fields of the two laser beams, employing the complete relativistic Lorentz force equation. The simulations are carried out on the fast temporal and spatial scales associated with the laser fields, including all components of the electromagnetic field. The particle equations of motion are integrated in a speed-of-light coordinate system in which the independent variables are $\zeta = ct - z$ and $\tau = t$. Boris' rotation is used for accurate finite differencing of the $\mathbf{v} \times \mathbf{B}$ force [23].

Two sets of results are discussed below. The first assumes a 4.5 MeV particle beam injector, with about 1 TW available in each laser beam. These parameters can be achieved using facilities available at the Naval Research Laboratory. The second employs a 50 MeV beam and is presented to demonstrate the scaling of the concept to higher energies. The numerical examples employ a laser beam with wavelength 1 μm and another at 1/2 μm. In practice this may be accomplished by splitting the beam from a 1 μm laser into two, frequency doubling one with a KDP (KH_2PO_4) crystal, and then recombining. The beams are phased such that $\psi_{0,2} - \psi_{0,1} = \pi/2$, although in practice this may be adjusted for optimization. The laser beam power, determined from the vector potential in Eq. (1), can be written as

$$P_j[\mathrm{TW}] = 0.0432(a_{0j} w_{0j}/\lambda_j)^2$$

in the paraxial limit. Similarly the peak (on-axis) intensity and electric field are given by

$$I_j[\mathrm{W/cm^2}] = 2.75 \times 10^{18}(a_{0j}/\lambda_j[\mu\mathrm{m}])^2, \qquad (17)$$

and

$$E_j[\mathrm{TV/m}] = 3.11 a_{0j}/\lambda_j[\mu\mathrm{m}], \tag{18}$$

respectively.

The results described below are designed to optimize the energy gain for given input electron beam and laser pulse parameters. Preliminary simulations in each case used a zero-emittance beam of particles, spread over a single laser wavelength along the axis, in order to obtain a rough guide for the laser beam parameters. Particles are injected along the positive z axis, well upstream of the focal point, where the laser intensity is small. Note that this is central to the VBWA concept: the particles enter and exit the combined laser fields at distances that are many Rayleigh ranges away from the region of high intensity. Consequently laser beam optical elements that are required to define the boundaries of the interaction region are not likely to be damaged. The appropriate initial condition is to set $\mathbf{u}_\perp = \mathbf{a}_\perp$ to mimic particles with zero transverse canonical momentum. These simulations were then followed by finite-emittance runs, where a convergent beam, consisting of 4000 particles, is injected along the axis. In this case the canonical momentum is zero: $\langle \mathbf{u}_\perp \rangle = \mathbf{a}_\perp$, where $\langle\ \rangle$ indicates an average over the particle distribution.

Prior to these studies it was felt that the laser beam parameters must be chosen so that the beat wave is sufficiently slow to be synchronous with the particles (i.e., $\beta_{ph} \approx \beta_z$) throughout the interaction. For the 4.5 MeV case, for example, this necessitates the Rayleigh range of the 1/2 μm beam to be much longer than that of the 1 μm beam, i.e., $Z_{R2} \gg Z_{R1}$ [see Eq. (7)]. Analysis of the numerical results, however, revealed that, due to diffraction, the phase velocity of the beat wave varied so rapidly in the focal region that it was not appropriate to attempt this synchronization. Further, phase space plots revealed no significant phase bunching, with particles dispersing apart at a rate that was closely related to their respective energies. It should be noted that, by employing disparate Rayleigh ranges, $Z_{R2} \gg Z_{R1}$, one is effectively wasting a significant portion of laser beam 2, since the beat wave is dominant only within a distance on the order of Z_{R1}. After performing simulations in which the above points were verified, the synchronization requirement was abandoned. Simulations were thereafter performed with equal Rayleigh ranges by appropriate choice of parameters.

(a) 4.5 MeV VBWA example. Table I lists the parameters for the 4.5 MeV case. Before proceeding with a description of finite-emittance simulations, we consider the ideal case. Figure 2 shows several plots for a zero-emittance beam, which illustrate some of the points made earlier. Here, a single particle is injected at $z=0$, $40Z_{R1}$ upstream of the focal point, and is followed to $40Z_{R1}$ past the focal point. The beat wave is expected to be significant within a few Rayleigh ranges on either side of the focus. The particle phase at the injection point is chosen for near-maximum energy gain. Figure 2(a) shows $1-\beta_{ph}$, as seen by the particle, as a function of z/Z_{R1}. Far upstream the beat wave is luminous. It speeds up slightly and then becomes subluminous for a short interval before and after the focus, becoming superluminous thereafter. Observe the rapid variation of the phase velocity in the vicinity of the focal point. This plot clearly shows the difficulty of maintaining synchronism between the particle and the beat wave. Figure 2(b), which shows $\beta_{ph}-\beta_z$, emphasizes this point and, in addition, shows that the beat wave is nowhere exactly synchronous with the particle.

TABLE I. Parameters for VBWA simulation with 4.5 MeV beam injected at $z=0$.

Injection energy	4.5 MeV
Normalized emittance ε_n	1.2 π mm mrad
Particle beam radius at waist	4 μm
λ_1	1 μm
Normalized vector potential $a_{0,1}$	1.3
Radiation waist $w_{0,1}$	4 μm
Focal point Z_{focus}	2 mm
Rayleigh range Z_{R1}	50 μm
Power (1 μm beam) P_1	1.16 TW
Power (1/2 μm beam) P_2	1.16 TW
Vector potential ratio $a_{0,2}/a_{0,1}$	$1/\sqrt{2}$
Waist ratio $w_{0,2}/w_{0,1}$	$1/\sqrt{2}$

Another important feature of the interaction is illustrated in Fig. 2(c), which shows the x components of the normalized vector potential and the normalized mechanical momentum. At the injection point the two variables are equal and they remain so right up to the focus, at which point the normalized momentum u_x (dashed line) receives a kick and deviates from a_x thereafter by a large and nearly constant amount. From Eq. (6) it would appear that this is caused by the transverse component of the ponderomotive force, which is large in this example due to the small focal spot size. Thus, the assumption of constant canonical momentum in Refs. [13] and [14] is valid only up to the focal point. In this connection the following two observations should be made. First, in the simulations the particle oscillation amplitude is not small compared to the laser spot size. This breaks the symmetry that is necessary for conservation of canonical momentum. Additionally, the analyses in Refs. [13] and [14] were based on the assumption of rapid particle quiver motion superposed on top of a slower ponderomotive motion. For the parameters here, however, the particle undergoes a few oscillations only in the interaction region and thus the decoupling into a small amplitude motion on top of a slow motion is not obtained.

Figure 2(d), which shows the transverse distance of the particle from the z axis, indicates a large sideways kick on passing through the focus. Examination of Eq. (7) shows that well after the focal point β_{ph} is a constant, as indicated in Fig. 2(a), provided r increases in proportion to $z-Z_{\mathrm{focus}}$. This dependence is precisely what is observed in Fig. 2(d). Since the displacement scales linearly with $z-Z_{\mathrm{focus}}$ it follows that the effect of the laser beams on the particles is akin to that of an impulse, delivered in the vicinity of the focal point. Consistent with this, Fig. 2(e) shows that the particle energy undergoes rapid changes in the focal region, plateauing at just under 8 MeV. (The energy gain can be improved significantly by employing a converging beam of particles, as described presently.)

We now proceed to describe the results of a realistic

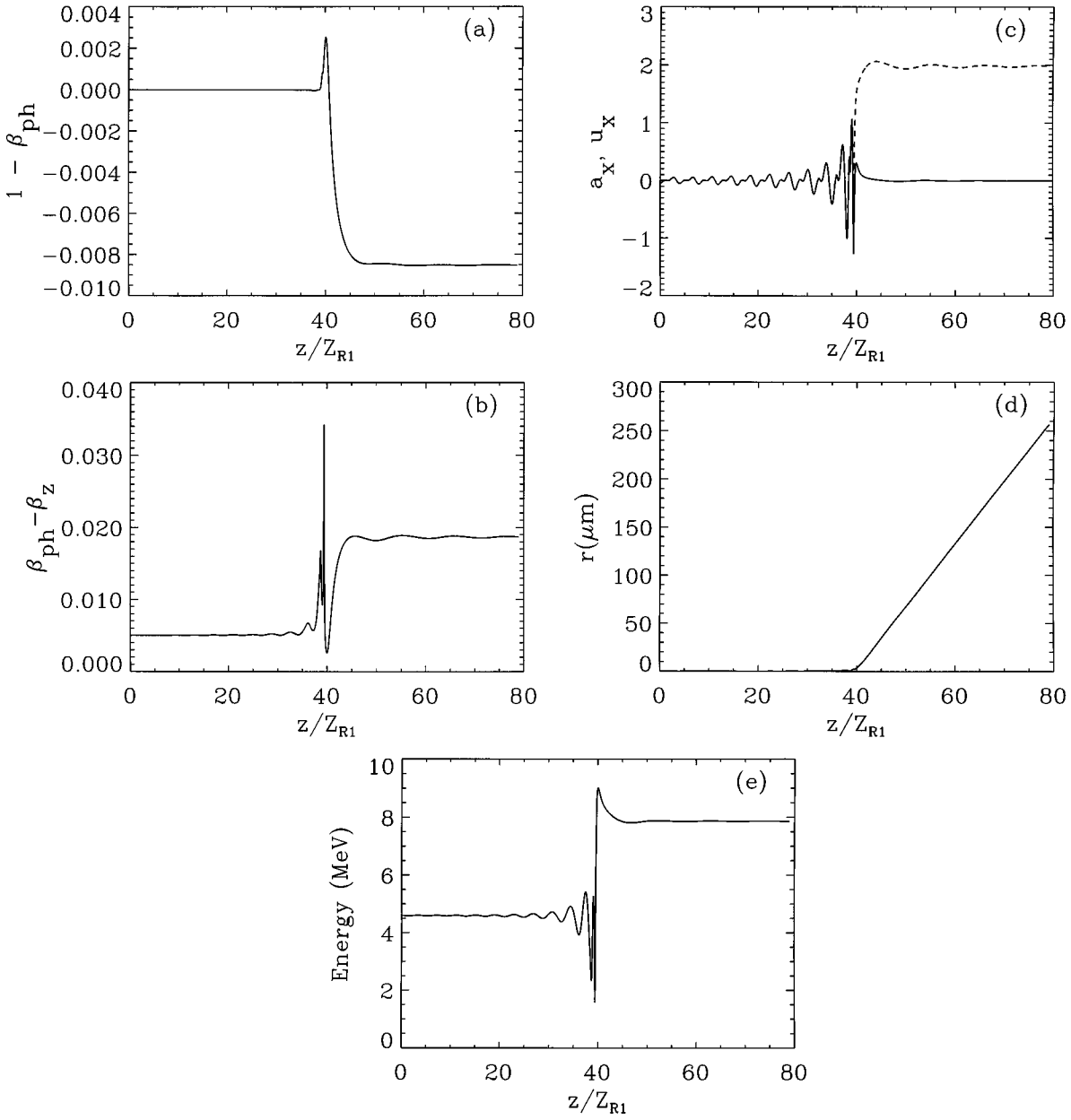

FIG. 2. Simulation results for a VBWA using a single particle with injection energy 4.5 MeV. The particle is injected on axis at $z=0$. The abscissa is measured in units of Rayleigh range, Z_{R1}, of laser beam 1. Laser beams come to focus $40Z_{R1}$ downstream of the injection point. Plots of (a) $1-\beta_{ph}$, (b) $\beta_{ph}-\beta_z$, (c) x components of normalized vector potential a_x (solid line) and normalized mechanical momentum u_x (dashed line), (d) radial displacement, and (e) energy as functions of axial distance.

simulation of a finite-emittance beam, with parameters as listed in Table I. Figure 3 shows the results. In order to approximately match the axial particle velocity with that of the beat wave, and to maximize a_{0j} it was necessary to choose a relatively small waist, $w_{0.1}=4$ μm. In practice the minimum waist for a Gaussian beam is given by $w_{\min}\approx f^{\#}\lambda$, where λ is the wavelength and $f^{\#}$ is the f number (defined for a lens that collects 99% of the laser beam) [24]. Thus a moderately sophisticated focusing element with f number close to 4 and a near-diffraction-limited beam must be employed to obtain the indicated laser waist. The relatively small f number and waist mean that the intensity and the field amplitude, evaluated with the aid of Eqs. (17) and (18), are very large at the focal point.

The computations employ a beam of noninteracting particles (i.e., with no space charge) with normalized root mean square (rms) emittance $\varepsilon_n=1.2\pi$ mm mrad. It is natural to arrange for the particle beam to come to focus at the same location as the laser beams. Commonly available optical elements for the particle beam line, such as bending magnets and quadrupoles, are suitable for focusing this beam down to an rms waist on the order of 4 μm and thus achieve a nearly optimal overlap of the optical and particle beams.

Interestingly, the convergent, finite-emittance particle

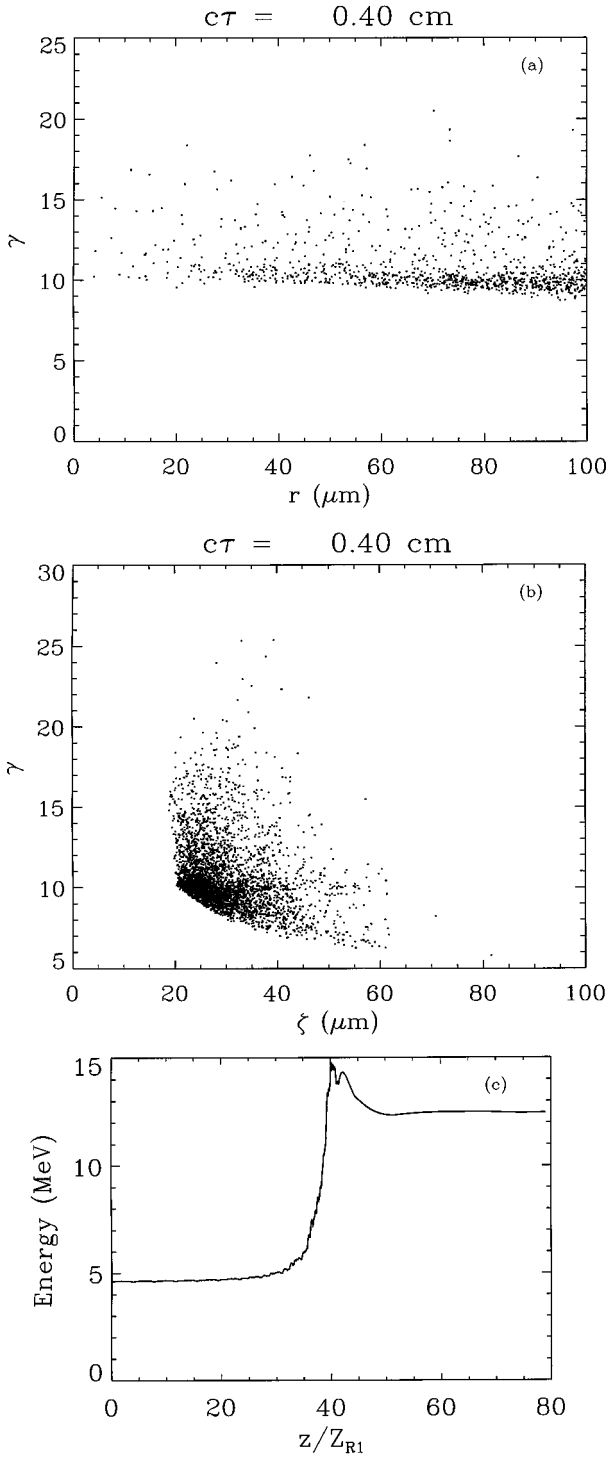

FIG. 3. Simulation results for a VBWA with injection of an initially converging 4.5 MeV finite-emittance beam. Particles are injected at $z=0$. Laser and particle beams come to focus $40Z_{R1}$ downstream of the injection point. Plots of (a) γ-r phase space and (b) longitudinal phase space (γ-ζ), at end of run, $c\tau=0.4$ cm. In the latter, the direction of beam propagation is towards the left. A plot of peak energy vs axial distance, with the abscissa measured in units of Rayleigh range, Z_{R1}, of laser beam 1, is shown in (c).

beam employed here has a characteristic that tends to enhance the energy gain in the VBWA configuration. As described earlier the transverse forces in the VBWA tend to scatter the particles after the focal point. With a convergent particle beam, coming to a focus at the point where the laser beams are in focus, it is found that there is a significant improvement in the net energy gain. Presumably this is because the convergence of the particles towards the focal point partially compensates for the scattering effect of the laser beams. The particles scatter away from the axis after the focal point isotropically.

TABLE II. Parameters for VBWA simulation with 50 MeV beam injected at $z=0$.

Injection energy	50 MeV
Normalized emittance ε_n	12 π mm mrad
Particle beam radius at waist	4 μm
λ_1	1 μm
Normalized vector potential $a_{0,1}$	6.5
Radiation waist $w_{0,1}$	4 μm
Focal point Z_{focus}	2 mm
Rayleigh range Z_{R1}	50 μm
Power (1 μm beam) P_1	29 TW
Power (1/2 μm beam) P_2	29 TW
Vector potential ratio $a_{0,2}/a_{0,1}$	$1/\sqrt{2}$
Waist ratio $w_{0,2}/w_{0,1}$	$1/\sqrt{2}$

Figure 3(a) shows the γ-r phase space, demonstrating that a small number of the high energy particles are close to the axis. The lack of significant phase bunching is demonstrated by the plot of the longitudinal phase space (γ-ζ, where $\zeta=ct-z$), shown in Fig. 3(b). Note that the particles, initially loaded over a longitudinal distance ~ 1 μm, are now spread over more than 50 μm. Observe that a small fraction of the particles are at the highest energies. Based on this and similar plots it is estimated that the fraction of particles with energy in excess 10 MeV is on the order of 1%. Finally Fig. 3(c) shows the peak energy of the ensemble of particles, along the interaction length. Observe that the energy rises up to $\sim$16 MeV in the vicinity of the focal point and then drops off, plateauing at $\sim$12.5 MeV. This final energy is 4 MeV higher than the case of on-axis injection in Fig. 2. Equation (16) predicts a peak energy of 17 MeV for $\Phi(Z_{\text{focus}})=-\pi/2$. The final dropoff can be reduced by injecting the particles into the interaction region at larger angles than in the present case. This tends to support our speculation that radial walkoff may be responsible for the phase detuning that leads to the drop in energy. In this connection, it must be noted that at the termination of the run, $z/Z_{RI}=80$, the spot sizes of the laser beams have expanded to $w_1=320$ μm and $w_2=226$ μm, respectively. That is, the highest energy particles are still within the laser spots. Even with the dropoff, one has a near tripling of the particle energy in a distance that is less than 4 mm. The peak acceleration gradient is on the order of 15 GeV/m.

(b) *50 MeV VBWA example.* Table II lists the parameters for the case with injection energy 50 MeV and Fig. 4 shows the results. Note that the laser beam power has been increased to 29 TW. This example is presented to indicate the potential of the VBWA at a higher injection energy. Alternatively it may be viewed as part of a multistage system

wherein each successive stage adds onto the beam a fraction of the desired total energy gain. It is apparent that to achieve a significant energy gain, for example to accelerate a particle beam from the MeV range to the GeV range, a multistage system is indispensable.

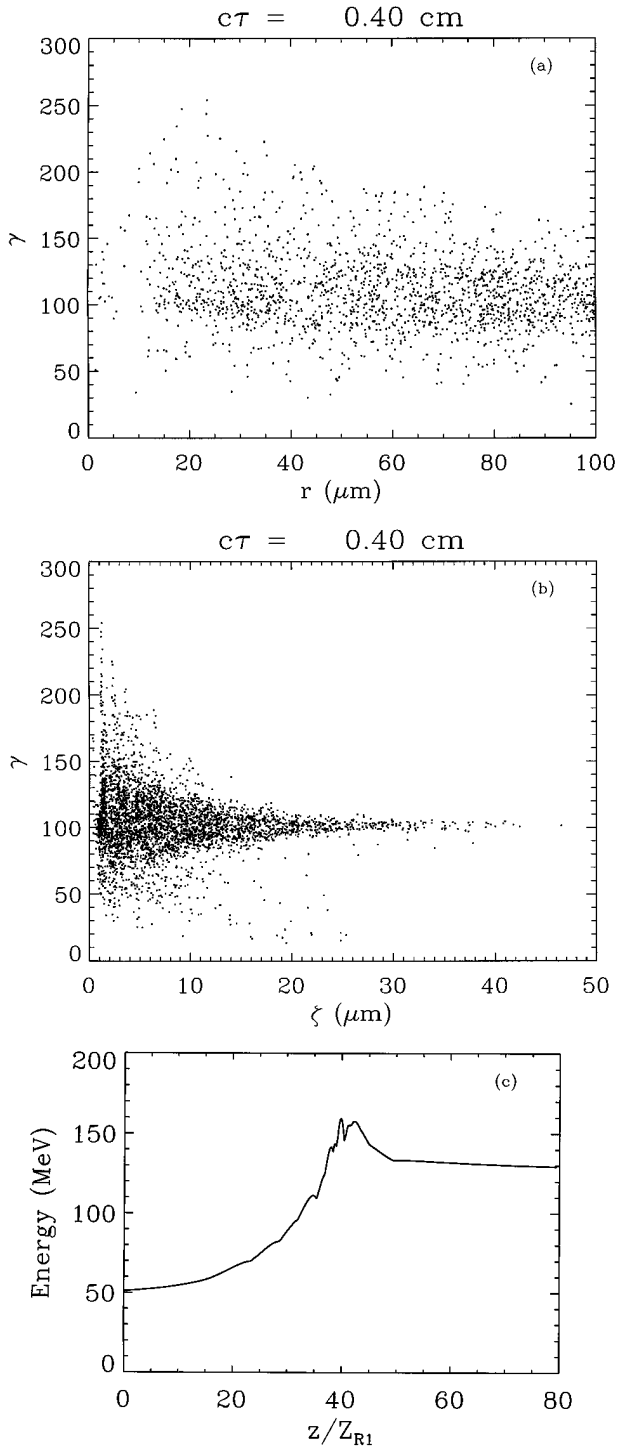

FIG. 4. Simulation results for a VBWA with injection of an initially converging 50 MeV finite-emittance beam. Particles are injected at $z=0$. Laser and particle beams come to focus $40Z_{R1}$ downstream of the injection point. Plots of (a) γ-r phase space and (b) longitudinal phase space (γ-ζ), at end of run, $c\tau=0.4$ cm. In the latter, the direction of beam propagation is towards the left. A plot of peak energy vs axial distance, with the abscissa measured in units of Rayleigh range, Z_{R1}, of laser beam 1, is shown in (c).

The particles are injected $40Z_{RI}$ upstream of the focus and followed to $40Z_{RI}$ past the focal point. Figures 4(a) and 4(b) show the γ-r phase space and the longitudinal phase space (γ-ζ), respectively, at the end of the run. A notable feature of Fig. 4(a) is that, in contrast to the 4.5 MeV case, the higher energy particles tend to be closer to axis. This is due to the fact that at higher energies the particles are stiffer and less susceptible to radial scattering by the ponderomotive force. By the same token a larger laser power, 29 TW per beam, is now required to nearly triple the energy, to ~150 MeV. The energy eventually levels off at ~130 MeV. Equation (16) predicts a peak energy of 140 MeV for $\Phi(Z_{\rm focus})=\pi/2$, although it is doubtful that any of the analytical estimates here are valid for values of $a_{0.1}$ or $a_{0.2}$ as large as in this example.

In closing it should be pointed out that single laser beam null tests, with $a_{0.2}=0$, were performed for both the 4.5 MeV and the 50 MeV examples. In both cases the energy was observed to change in the vicinity of the focal point, returning to its original value far downstream. No significant net acceleration was observed with a single laser beam.

V. SUMMARY AND CONCLUSION

Simulations reveal some key characteristics of the VBWA. First, in practice, the variation of the phase velocity in the focal region leads to rapid detuning of particles from the beat wave. Second, the interaction is in the nature of an impulse delivered to the particles in the focal region. Third, particles are scattered radially on passing through the focus. As a result, slippage and walkoff tend to limit the acceleration gradient of the VBWA. It may be possible to reduce the radial scattering by using larger laser spot sizes. The examples in this paper assume the fundamental Gaussian laser profile, with the peak intensity on the axis and, therefore, a net defocusing radial force. One can envisage the use of radial profiles that exhibit a minimum on the axis, such as a combination of higher order Gaussian modes, that do not lead to particle scattering.

Previous models of the interaction have been extended to obtain improved estimates for the energy gain. Further, through simulations it is demonstrated that the energy gain can be improved significantly by employing a converging particle beam that is focused at the same location as the laser beams. Thus, it is shown that one can, with readily available state-of-the-art equipment, design a VBWA that will have an acceleration gradient far in excess of what will be achievable with conventional radio-frequency technology. Finally, it should be emphasized that, since the vacuum beat wave accelerator is limited neither by material damage nor by annihilation of antiparticles, it has clear advantages *vis-a-vis* the inverse Cerenkov and the plasma wakefield accelerator concepts.

ACKNOWLEDGMENTS

The authors have benefited from extensive discussions with Dr. J. L. Hirshfield and Dr. A. Ganguly. This work was supported by the Department of Energy and the Office of Naval Research.

[1] *Advanced Accelerator Concepts*, edited by P. Schoessow, AIP Conf. Proc. No. 335 (AIP, New York, 1995); IEEE Trans. Plasma Sci. **PS-24** (1996); special issue on second generation plasma accelerators, edited by T. Katsouleas and R. Bingham; E. Esarey, P. Sprangle, J. Krall, and A. Ting, IEEE Trans. Plasma Sci. **PS-24**, 252 (1996).

[2] Y. Kitagawa, T. Matsumoto, T. Minamihata, K. Sawai, K. Matsuo, K. Mima, K. Nishihara, H. Azechi, K. A. Tanaka, H. Takabe, and S. Nakai, Phys. Rev. Lett. **68**, 48 (1992).

[3] C. E. Clayton, K. A. Marsh, A. Dyson, M. Everett, A. Lal, W. P. Leemans, R. Williams, and C. Joshi, Phys. Rev. Lett. **70**, 37 (1993).

[4] M. Everett, A. Lal, D. Gordon, C. E. Clayton, K. A. Marsh, and C. Joshi, Nature **368**, 527 (1994).

[5] K. Nakajima, D. Fisher, T. Kawakubo, H. Nakanishi, A. Ogata, Y. Kato, Y. Kitagawa, R. Kodama, K. Mima, H. Shiraga, K. Yamakawa, T. Zheng, Y. Sakawa, T. Shoji, Y. Nishida, N. Yugami, M. Downer, and T. Tajima, Phys. Rev. Lett. **74**, 4428 (1995).

[6] C. A. Coverdale, C. B. Darrow, C. D. Decker, W. B. Mori, K. C. Tzeng, K. A. Marsh, C. E. Clayton, and C. Joshi, Phys. Rev. Lett. **74**, 4659 (1995).

[7] A. Modena, Z. Najmudin, A. E. Dangor, C. E. Clayton, K. A. Marsh, C. Joshi, V. Malka, C. B. Darrow, C. Danson, D. Neely, and F. N. Walsh, Nature **337**, 606 (1995).

[8] D. Umstadter, S. Y. Chen, A. Maksimchuk, G. Mourou, and R. Wagner, Science **273**, 472 (1996).

[9] A. Ting, C. I. Moore, K. Krushelnick, E. Esarey, P. Sprangle, R. H. Hubbard, H. R. Burris, R. Fischer, and M. Bain, Phys. Plasmas (to be published).

[10] J. A. Edighoffer and R. H. Pantell, J. Appl. Phys. **50**, 6120 (1979).

[11] M. O. Scully and M. S. Zubairy, Phys. Rev. A **44**, 2656 (1991).

[12] E. J. Bochove, G. T. Moore, and M. O. Scully, Phys. Rev. A **46**, 6640 (1992).

[13] P. Sprangle, E. Esarey, J. Krall, and A. Ting, Opt. Commun. **124**, 69 (1996).

[14] E. Esarey, P. Sprangle, and J. Krall, Phys. Rev. E **52**, 5443 (1995).

[15] Y. C. Huang, D. Zheng, W. M. Tulloch, and R. L. Byer, Appl. Phys. Lett. **68**, 753 (1996); Y. C. Huang and R. L. Byer, *ibid.* **69**, 2175 (1996).

[16] P. Sprangle, E. Esarey, and J. Krall, Phys. Plasmas **3**, 2183 (1996).

[17] F. V. Hartemann, S. N. Fochs, G. P. LeSage, N. C. Luhmann, G. J. Woodworth, M. D. Perry, Y. J. Chen, and A. K. Kerman, Phys. Rev. E **51**, 4833 (1995).

[18] E. Esarey, P. Sprangle, M. Pillof, and J. Krall, J. Opt. Soc. Am. B **12**, 1695 (1995).

[19] J. D. Lawson, IEEE Trans. Nucl. Sci. **NS-26**, 4217 (1979).

[20] R. B. Palmer, in *Frontiers of Particle Beams*, Vol. 296 of *Lecture Notes in Physics*, edited by M. Month and S. Turner (Springer-Verlag, Berlin, 1988), p. 607.

[21] M. D. Perry and G. Mourou, Science **264**, 927 (1994).

[22] A. E. Siegman, *Lasers* (University Science Books, Mill Valley, CA, 1986), Sec. 17.4.

[23] C. K. Birdsall and A. B. Langdon, *Plasma Physics Via Computer Simulation* (McGraw-Hill, New York, 1985), Chaps. 4 and 15.

[24] In Ref. [22], Sec. 17.2.